Preprint Title Green synthesis of carbon quantum dots from biomass with down and upconversion luminescence for methylene blue degradation

Authors Dalia H. Chavez-Garcia, Mario H. Guzman, Viridiana Sanchez and Ruben D. Cadena-Nava

Publication Date 20 Feb. 2024

Article Type Full Research Paper

ORCID® iDs Dalia H. Chavez-Garcia - https://orcid.org/0000-0002-1258-7238; Mario H. Guzman - https://orcid.org/0000-0002-0873-4936; Viridiana Sanchez - https://orcid.org/0009-0002-4517-3856; Ruben D. Cadena-Nava - https://orcid.org/0000-0001-8428-6701

Green synthesis of carbon quantum dots from biomass with down and upconversion luminescence for methylene blue degradation

Dalia Chávez-García [1,*], Mario Guzman[1,**], Viridiana Sanchez[1], Ruben D. Cadena-Nava[2,]***

[1] Centro de Enseñanza Técnica y Superior (CETYS), Ensenada, B.C., México

[2]Centro de Nanociencias y Nanotecnología (CNYN), Universidad Nacional Autónoma de México (UNAM), Ensenada, B.C., México

***Corresponding author:**

Email: dalia.chavez@cetys.mx.

Web of Science Researcher ID: T-3640-2019

ORCID ID: 0000-0002-1258-7238.

** ORCID ID: 0000-0002-0873-4936

*** ORCID ID: 0000-0001-8428-6701

ABSTRACT

Water pollution, driven by the discharge of synthetic dyes from industries like textiles, remains a global threat to human health. Methylene blue, a common dye in the textile sector, exacerbates this issue. In response, this study presents a novel approach to mitigate water pollution by synthesizing nanomaterials using biomass-derived (grapes and watermelon) carbon quantum dots (CQDs). Employing the hydrothermal method at temperatures ranging from 80°C to 160°C for 1 to 24 hours, CQDs were successfully synthesized using watermelon shell and grape pomace as organic precursors. Characterization techniques, including UV-Visible spectra, Fourier transform infrared spectroscopy (FTIR), dynamic light scattering (DLS), and luminescence spectroscopy, verified the quality of the CQDs. Degradation tests on methylene blue were conducted separately under sunlight and incandescent focus light irradiation, assessing catalytic activity at 20-minute intervals over a 2-hour period. The CQDs (1-10 nm) exhibit optical properties including upconversion and downconversion luminescence. This CQDs shown an effective photocatalytic activity in methylene blue degradation under sunlight. The straightforward and cost-effective synthesis process suggests the potential for scalable production of catalytic nanomaterials for synthetic dye degradation.

KEYWORDS

Carbon dots, catalysis, methylene blue, biomass, photoluminiscence

INTRODUCTION

The textile industry is characterized by its high consumption of water, energy, and chemical reagents. For example, a pair of indigo-dyed pants requires at least 42 liters of water to be manufactured, in addition to the approximately 21 liters of water needed each time they are washed at home. The textile industry strives to make its dyes increasingly resistant, with high chemical and photocatalytic stability, to ensure the quality of its products. Therefore, dyes are designed to be resistant to light exposure, detergents, and cleaning products, making them much more difficult to remove. On the other hand, when these colorants are released into rivers, seas, and lakes, they can cause pollution problems such as chemical oxygen demand, toxicity, and reduced light penetration, affecting living organisms, primarily aquatic life. This has led the textile industry to become one of the major contributors to water pollution [1].

To address this issue, it is important for the textile industry to take steps to reduce its environmental impact. This may include adopting more sustainable practices in water and energy use, as well as developing and using more environmentally friendly dyes. Implementing wastewater treatment processes can also help reduce the amount of contaminants released into the environment. Ultimately, it is essential for the textile industry to take responsibility and seek solutions that minimize its impact on natural resources and the environment as a whole. Embracing more sustainable practices and developing eco-friendly technologies are key to achieving a balance between textile production and environmental preservation.

There are various conventional techniques available for wastewater treatment; however, due to the high resistance of these colorants, they cannot be effectively eliminated using these methods. Conventional techniques may only reduce the level of contaminants, and more complex and environmentally unfriendly processes are required to deal with these persistent colorants. As a result, there is a growing need for the development and implementation of more advanced and sustainable technologies for the treatment of wastewater from the textile industry. These technologies should be capable of efficiently removing the resistant colorants and other pollutants while minimizing their impact on the environment.

In recent years, researchers and engineers have been exploring innovative approaches for wastewater treatment, such as advanced oxidation processes, nanotechnology-based methods, and biological treatment systems. These

techniques show promising results in effectively degrading and removing pollutants, including resistant dyes, from wastewater. It is crucial for the textile industry to invest in research and development to adopt these environmentally friendly and efficient technologies. By doing so, they can significantly reduce their environmental footprint and contribute to the preservation of clean water resources for a sustainable future.

In this research, the investigation and synthesis of carbon quantum dots (CQDs) are carried out through a hydrothermal method, chosen for its ease of production, low cost, and scalability. Biomass derived from watermelon peels and waste from the local wine industry (grape pomace) are utilized to produce the material. The goal is to evaluate the potential of the CQDs as catalysts in the photocatalysis technique for degrading methylene blue dye present in industrial wastewater.

Photocatalysis has emerged as one of the most environmentally friendly methods for water purification. It offers the advantage of destroying contaminants by accelerating a chemical reaction through a catalyst activated by light radiation, compared to traditional methods that simply transfer contaminants from one phase to another. Previous studies have reported the use of carbon quantum dots as catalysts in photocatalytic activity, such as the hybrid C/TiO_2 catalyst. However, despite being called green synthesis, some studies involve the use of a variety of costly equipment, contradicting the notion of a truly green approach [2,3].

Carbon dots (CQDs) have gained significant attention due to their easy synthesis, good solubility, photostability, non-toxic properties, and versatile applications. Various synthesis methods have been employed, including both top-down approaches such as arc discharge, plasma fabrication, laser ablation, and bottom-up methods such as hydrothermal, microwave, chemical oxidation, and pyrolysis [4–10]. Green synthesis using biomass as a carbon-rich resource [11], has become increasingly popular, with materials such as eggshells [12,13], papaya peel [14], lemon peel [15], banana juice [16], orange juice [17], pine tannin [18], and candle soot [19] being utilized.

CQDs find applications in sensing[15], cell imaging[20], drug delivery[21], photocatalysis [22], energy conversion, and storage[23], among others. The advantage of bottom-up synthesis methods is that they are easier, eco-friendly, and cost-effective, and CQDs synthesized using these methods can exhibit relatively high quantum yields (QY), resulting in intense luminescence compared to top-down methods, although they may have an amorphous structure. In this research, biomass from watermelon shell and grape pomace waste from the Baja California wine industry in Mexico was used as the carbon source. The hydrothermal method was employed with three solvents: urea, nitric acid, and water. Samples subjected to a chemical oxidation process with nitric acid during synthesis exhibited better catalytic activity.

CQDs typically exhibit luminescence properties, with emission peaks in the blue region between 450 and 500 nm [24,25]. The emission peaks may vary depending on the solvent used, as reported by Zhang *et al.* [26], who used polystyrene foam waste and organic solvents. Some authors have reported upconversion emission, such as Cheng *et al.* [27], who synthesized CQDs from walnut shells and observed emission peaks between 490 and 500 nm when excited by long wavelengths from 600 to 800 nm. In this research, upconversion emission was observed from the CQDs excited at 900 nm, with emission peaks at 727 nm, as well as downconversion emission in the blue region. The photocatalytic activity of CQDs in methylene blue degradation has been reported by several authors [12,14,28], including Wang *et al.* [13], who synthesized CQDs from eggshells and demonstrated methylene blue degradation under sunlight irradiation.

In this research, samples synthesized with nitric acid exhibited the best catalytic activity in methylene blue degradation, while those prepared with water as a solvent did not show significant catalytic activity. The samples were also characterized using UV-Visible spectra, Fourier transform infrared spectroscopy (FTIR), dynamic light scattering (DLS), and photoluminescence spectroscopy (PL). The utilization of biomass as a carbon source offers great opportunities due to its abundance in nature and the wide range of sources available, which exhibit good luminescent and catalytic properties.

By focusing on the hydrothermal synthesis method using biomass-derived precursors, this research aims to develop a more sustainable and cost-effective approach for producing CQDs as catalysts in the photocatalysis process. The use of watermelon peels and grape pomace as raw materials contributes to waste valorization and promotes a circular economy concept. The ultimate goal is to provide a greener and more efficient solution for wastewater treatment in the textile industry, reducing environmental impact and conserving clean water resources. This research represents a significant step towards addressing water pollution caused by the textile industry and highlights the potential of nanotechnology in developing sustainable solutions.

Experimental

Materials/Material synthesis

The synthesis of CQDs involved the utilization of biomass-derived precursors. The method employed was based on the hydrothermal approach reported by Sun *et al.* [1,26,29] with modifications in terms of precursor selection and chemical conditions.

Two organic materials, watermelon rind and grape pomace, were used as the precursors, which were obtained from waste generated by the local wine industry. Initially, small pieces of the biomass were cut and placed on

metal trays, followed by drying in a convection oven at 60°C. Subsequently, the dried precursors were individually crushed in a mortar until they formed a fine powder. Additionally, four different synthesis schemes were proposed, involving modifications in the chemical conditions of the precursor solution.

In a typical synthesis 50 ml of deionized water was mixed with 0.5 g of biomass precursor powder (dispersion A) and stirred for 10 minutes. Then, 1.0 g of urea (hydrolizing agent under hydrotermal conditions) diluted in 50 ml of deionized water to form a homogeneous solution (solution B) and then mixed with the dispersion A. The final mixture was stirred for an additional 10 minutes. Subsequently, the mixture was transferred to a Teflon lined stainless steel autoclave, which was sealed under pressure using a manual press. The autoclave was then placed in a convection oven and maintained at 100°C for two hours. After the specified time had elapsed, the autoclave was allowed to cool and the solution was retrieved After the synthesis, the solutions were filtered through a Buchner funnel equipped with a 200 nm nylon membrane from the Whatman brand[30] and centrifuged at 15000 rpm for 20 minutes as depicted in Figure 1.

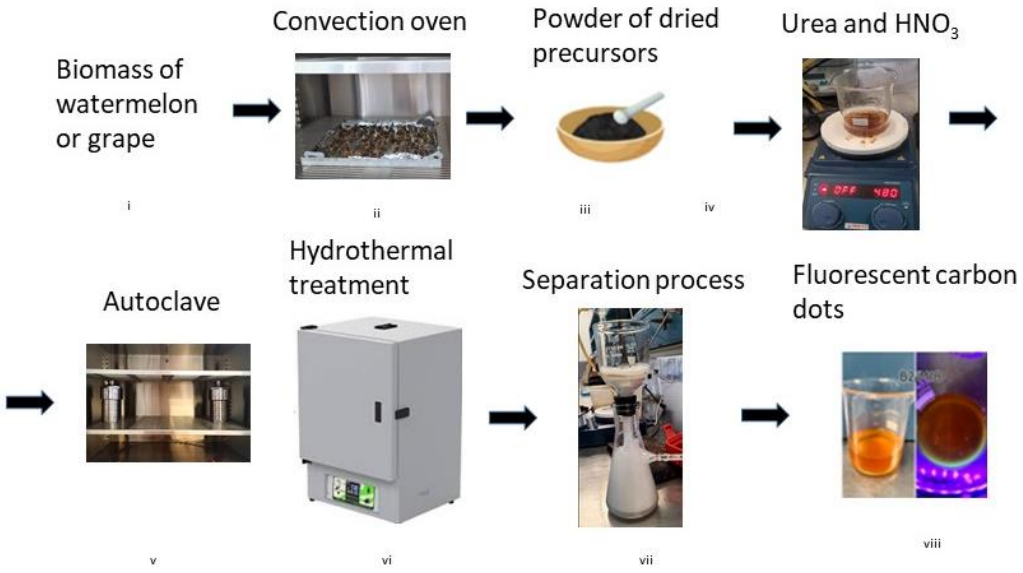

Figure 1. CQDs synthesis process assisted by the hydrothermal method.

The process previously described was repeated modifying the chemical condition varying solution B as it follows: 1.0 of urea in 50 ml of deionized water (samples M1 and M5); ii) 1.0 g of urea and 5.0 ml of 2.5 ml of nitric acid (69 % v/v) in 50 ml of deionized water (samples M2 and M6); iii) 2.5 ml of nitric acid (69 % v/v) in 50 ml of deionized water and (samples M3 and M7) iv) 50 ml of deionized water (M4 and M8). Samples M1, M2, M3 and

M4 were prepared using grape pomace peel as biomass precursor, and samples M5, M6, M7 and M8 were prepared using watermelon peel as biomass precursor.

Characterizations

UV-Vis spectroscopy

To determine the optoelectronic characteristics of the synthesized CQDs, UV-Vis absorption spectra were measured using a Thermo Scientific Evolution 220 spectrophotometer. The CQDs were dissolved in deionized water at a ratio of 1:10 and the measurements were taken in the range of 200 to 800 nm. A 1 cm pathlength quartz cell was used for the measurements, and deionized water was used as the blank in the measurement to account for background signals.

FTIR spectroscopy

Fourier transform infrared spectra (FTIR) were measured on Spectrum Two FT-IR/Sp 10 S/W spectrometer (USA) with a $LiTaO_3$ type detector, the wavelength used was ranging from 450 cm^{-1} to 4000 cm^{-1}.

Dynamic light scattering

The size distribution of the synthesized CQDs was determined using dynamical light scattering (DLS) technique, which relies on the measurement of the hydrodynamic radius of the particles. The CQDs were analyzed by Malvern NanoSizer ZP instrument. The samples were diluted in deionized water to prevent signal saturation. Multiple measurements (at least 3) were performed for each sample to ensure reliable and accurate measurements. A quartz cell with a 1 cm path length was used for the DLS measurements using a Malvern Zeta-sizer equipment model 7.2.

Photoluminescene spectroscopy

The PL spectra of the samples was performed with a Agilent Cary Eclipse fluorescence spectrophotometer. It consists of two Czerny-Turner slits (excitation and emission) with a double monochromator, a continuous emission xenon light source between 190 nm and 900 nm; the samples were analyzed with a wavelength excitation of 350 nm and 900 nm, all the samples were analyzed in aqueous medium, the samples were dispersed in deionized water before the analysis.

Degradation of methylene blue

The photodegradation tests were conducted separately using sunlight and incandescent light (tungsten-halogen lamp 40 W) to evaluate their respective efficiency in the degradation process. To initiate the catalytic activity process, each CQDs sample was individually applied to the degradation of the methylene blue dye. The UV-Vis absorption spectrum of the dye was monitored using a Thermo Scientific Evolution model 220 spectrophotometer with a 1 cm path length quartz cell.

To evaluate the photocatalytic activity of the CQDs, 17.5 ml of a 10 ppm methylene blue solution was placed in a baker under constant stirring. Subsequently, 2.5 ml of the CQDs suspension was added to the solution. Before initiating the light irradiation, the suspension was stirred for 20 minutes at 400 rpm in a dark environment to ensure proper dispersion of the CQDs in the aqueous media and the adsorption of the dye on the CQDs surface. After the 20-minute stirring period, the absorbance of the solution was measured using the spectrophotometer in the wavelength range of 250 to 800 nm. This measurement marked the start of the photodegradation reaction under light radiation. In the case of tests conducted with incandescent light, a lamp was used as the light source, placed approximately 10 cm away from the solution, and the reaction was allowed to proceed for 100 minutes.

During the degradation tests, both sunlight and incandescent light were used, and the solution was continuously agitated. The absorbance of the solution was measured at 20-minutes intervals to monitor the progress of the degradation reaction. Figure 2 illustrates the process of the degradation tests as described above.

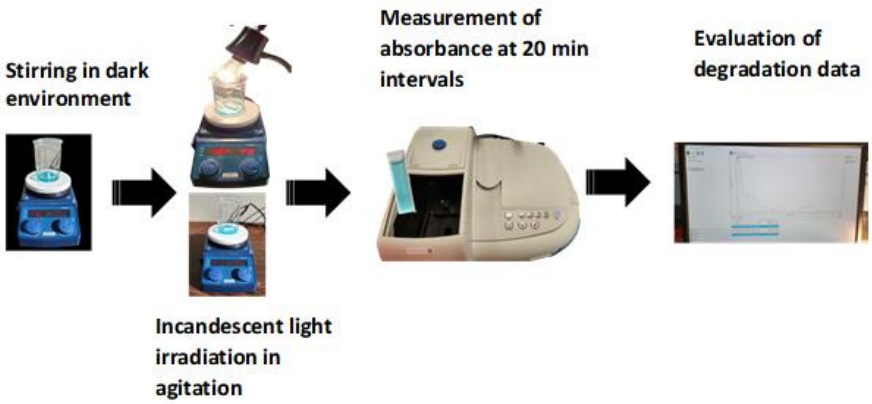

Figure 2. Diagram of the degradation process of the methylene blue dye.

These tests were repeated using each of the four grape pomace samples and four watermelon peel samples for evaluation. The pH value of the solution was kept constant at 7.

Results and discussion

UV-Vis spectroscopy

We used UV-Vis spectroscopy to analyze the optoelectronic properties of the eight samples of the CQDs synthesized by the hydrothermal method. All the samples were diluted in deionized water to adjust the absorbance, the figure 3 shows the CQDs synthesized from a) grape pomace peel and, b) watermelon peel. It is observed that for each of the samples its maximum absorption peak is approximately 350 nm of wavelength which corresponds to the n-π* transitions present in unsaturated compounds with heteroatoms (carbonyl groups) but also a tail of absorbance is noticed in the visible range [31,32]. The samples M6 and M7 (Figure 3b and c) present a relatively symmetrical band also centered at 350 nm with a higher intensity for sample M6, both samples were prepared using an oxidation process with nitric acid prior to hydrothermal treatment, to break the structure of the carbohydrate used. On the other hand, samples M5 and M8 exhibit an asymmetric behavior in their absorption band centered around 340 nm, the difference can be associated with the polydispersity in the size of the CQDs due to the absence of acid oxidation processes, being in this case the hydrothermal treatment is solely responsible for the formation of CQDs. This same condition was observed when modifying the type of precursor (grape pomace), however, in the case of the samples prepared from grape pomace a considerably less intense band is observed for the systems prepared with Urea (M1 and M5), this possibly associated with a low production of CQDs (Figure 3a).

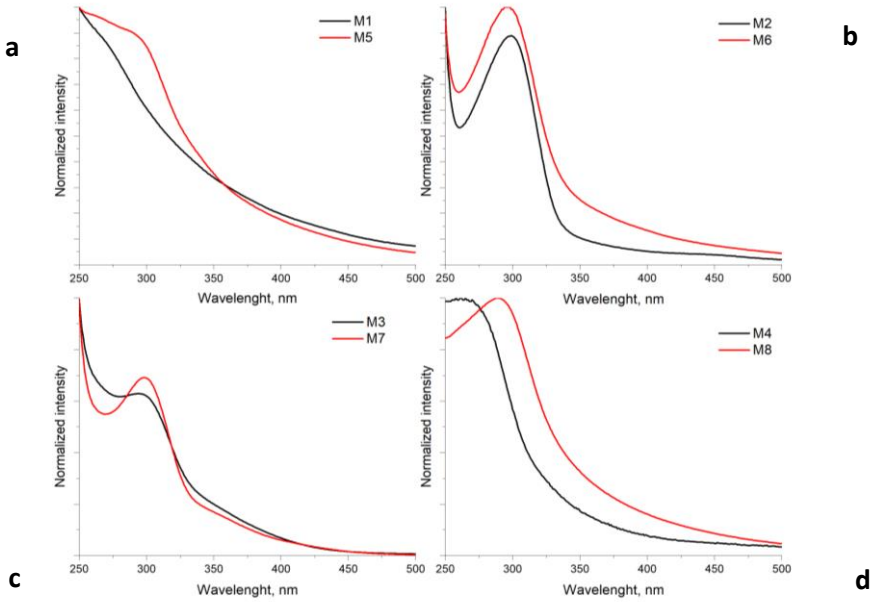

Figure 3. UV-Vis absorbance spectra of the samples of CQDs synthesized with a) Urea (M1 grape and M5 watermelon), b) Urea and nitric acid (M2 grape and M6 watermelon), c) Nitric acid (M3 grape and M7 watermelon) and d) Deionized water M4 grape and M8 watermelon)

Dynamic Light Scattering

Figure 4 shows the size distribution of the QCDs by dynamic light scattering (DLS). Notably, samples M2, M3, M6, and M7, incorporating acid during synthesis, exhibit sizes within the range of 1 to 10 nanometers, characteristic sizes of quantum dots. In contrast, samples M1 and M5, synthesized with urea, display larger sizes ranging from 10 to 100 nm, while samples M4 and M8, synthesized using only water, have sizes close to 100 nm. It is important to note that the samples prepared using grape pomace peel as a biomass source produced smaller particle sizes compared to those prepared with watermelon peel under identical synthesis conditions. The size distribution determined by DLS underlines the influence of biomass source and synthesis parameters on the resulting CQD dimensions.

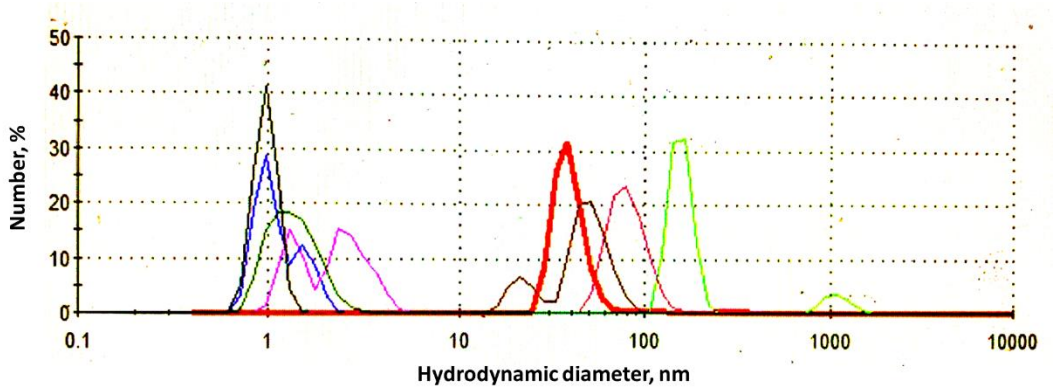

Figure 4. Size distribution of the CQDs by dynamical light scattering. Samples M1, – M2, – M3, – M4, – M5, – M6, – M7 and –M8.

Fourier Transformed Infrared Spectroscopy

The surface chemical groups of the samples were analyzed using FTIR spectroscopy. Figure 5a displays the FTIR spectrum of the CQDs synthesized with grape pomace. Since the systems were prepared in water, some of the signals may have been shielded. In the spectrum, the absorption bands at 3350 cm^{-1} correspond to the OH vibrations and N-H bonds, likely originating from water derived from the oxidation process. These bands are characteristic of the hydroxyl groups present in the acid structure. The peaks around 1600 cm^{-1} fall within the C-O range. The samples synthesized with nitric acid oxidation exhibit an additional peak at 1400 cm^{-1}, associated with C-H and C-N bending vibrations, indicating the introduction of nitrogen atoms and oxygen-containing groups. The oxidation process enhances the solubility of CQDs in water. The spectrum also shows low-intensity signals in the range of 1800 to 2500 cm^{-1}, which are characteristic of aromatic compounds [25,31].

In Figure 5b, the FTIR spectrum of the CQDs synthesized from watermelon peel is shown. Similar characteristics to the grape pomace CQDs samples can be observed, especially for sample M7, which was also synthesized using nitric acid (similar conditions as sample M3). However, the characteristic carbon-nitrogen groups of the acid, indicated in the green oval, are not observed in sample M7. This could be attributed to the complete consumption of these groups during the treatment, resulting in their signals not being detected in this analysis.

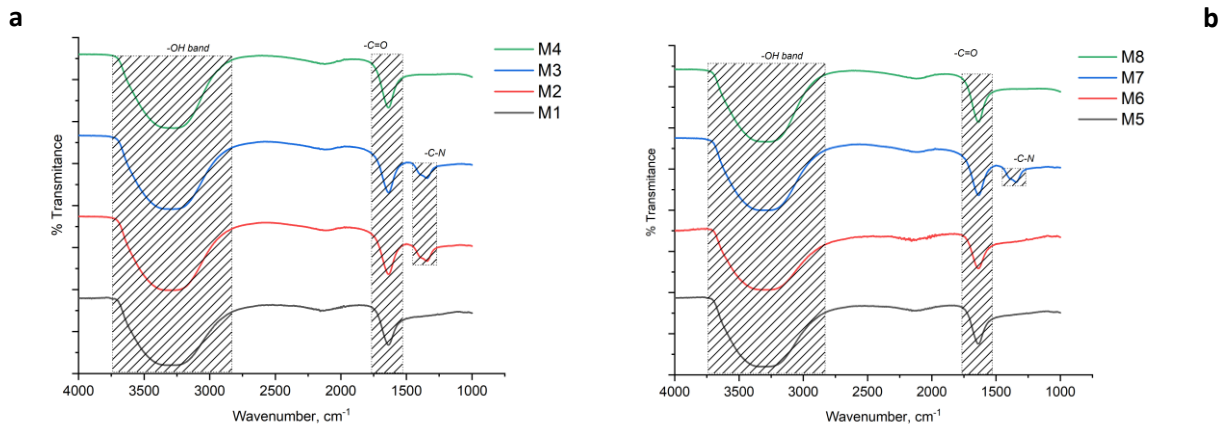

Figure 5. FTIR of a) grape pomace peel with carbonyl peaks, carbon-nitrogen bonds, OH vibrations and some overtones of the benzene ring can be observed, and the b) watermelon peel shows characteristics similar to the grape pomace samples are evident.

Photoluminescence spectra

Investigating the underlying origin and mechanisms governing the multi-fluorescence behavior of carbon dots has garnered significant interest in recent times. Diverse research groups have delved into the fluorescence characteristics of CQDs, presenting varied mechanistic explanations. These encompass phenomena like recombination of electron-hole pairs, quantum effects, surface functional groups, surface states, molecular states, and fluorophores exhibiting differing degrees of π-conjugation. Generally, CQDs comprise a carbon-core domain and surface domains [33].

In the context of PL processes in CQDs, the emission of fluorescence is intriguing and often associated with the presence of surface defects. Various researchers have highlighted the role of radiative recombination of electron-hole pairs and the influence of functional groups within the carbon network in driving the fluorescence phenomenon [27,34,35]. Furthermore, carbon nanomaterials exhibiting fluorescence, such as carbon oxide dots, exhibit a diverse array of structural elements, including sp^2 carbon hybridization or partial hybridization commonly observed in carbon oxide dots [34,36].

The PL downconversion spectra of the CQDs synthesized from grape pomace and watermelon peel are shown in Figures 6a and 6b, respectively. All samples were excited at a wavelength of 350 nm, and the emission was observed in the range of 440-450 nm. The samples prepared with urea, namely M1 and M5, exhibited higher intensity in the PL spectra. The PL emission of CQDs can also be influenced by the surrounding acidic conditions,

potentially leading to fluorescence quenching. Notably, the sample M3 synthesized using nitric acid demonstrated lower PL intensity, possibly due to such quenching effects under acidic conditions[37].

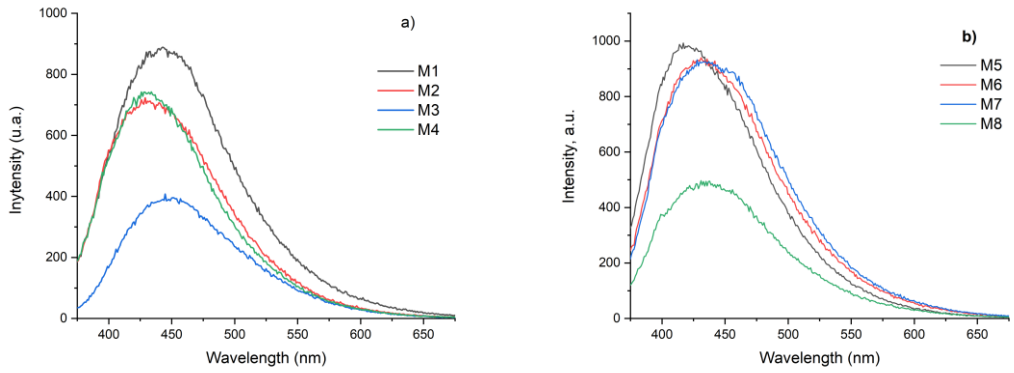

Figure 6. PL spectra, the samples were excited with 350 nm, the graphics corresponds to a) grape pomace peel and, b) watermelon peel. excitation wavelength at 900 nm.

The upconversion luminescence observed in Figure 7 shows a phenomenon where the emitted fluorescence has a shorter wavelength than the excitation wavelength. This is different from the downconversion luminescence, where the excitation occurs in the UV region and the emission takes place in the visible spectrum. Unlike downconversion luminescence, upconversion luminescence does not require high photon density and can occur under normal excitation conditions [36]. Several authors have reported the existence of upconversion carbon dots (CDs). For example, Zhu *et al* [34] demonstrated upconversion CDs, while Zhuo *et al* [38] reported graphene CDs with upconversion luminescence. The theoretical framework proposed for upconversion photoluminescence centers on the concept of the quantum confinement effect (QCE). In this scenario, electrons migrate from the lowest unoccupied molecular orbital (LUMO) to the highest occupied molecular orbital (HOMO) when the excitation wavelength surpasses 600 nm. This process is elucidated in Figure 7 [27,39]. In figure 8 is observed the upconversion PL of all the samples, with excitation at 900 nm and emission in the visible spectra at 720-730 nm. The samples from grape pomace were the ones with more emission than the samples from watermelon, similar behavior as the downconversion process.

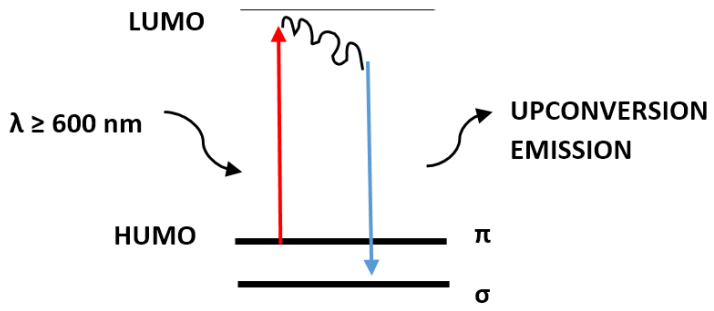

Figure 7. The upconversion process of the quantum confinement effect.

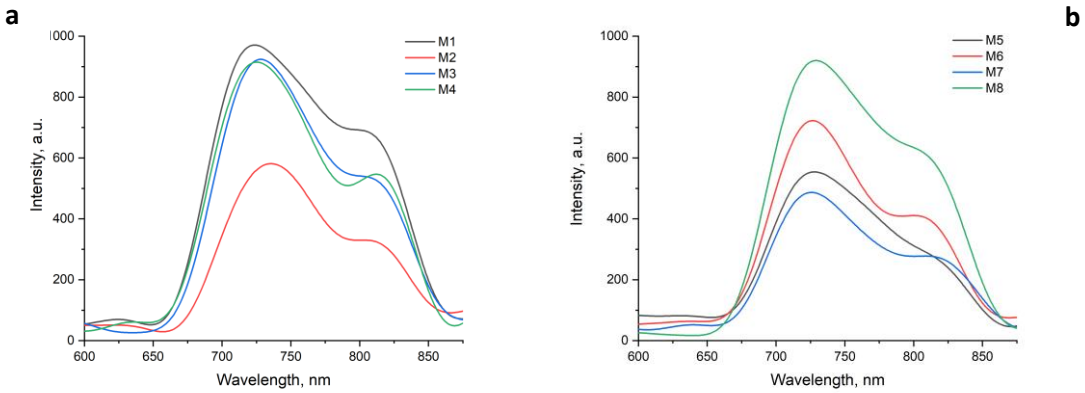

Figure 8. Upconversion PL of the samples, the graphics corresponds to grape pomace peel (M1 to M4) and watermelon peel (M5 to M8).

Photocatalytic activity

To carry out the evaluation of the catalytic activity with each of the obtained samples, the curves were first fitted using the calculation of the reaction rate with the pseudo-first-order method.

Calculation of the reaction rate constant

The calculation of the reaction rate constant can be performed using the first-order kinetic model. The first-order rate equation is given by:

$$\ln\left(\frac{Co}{C}\right) = kt$$

Where: C_0 is the initial concentration of the reactant (methylene blue dye), C is the concentration of the reactant at time t, k is the first-order rate constant, and t is the reaction time.

The value of the kinetic rate constant (k) was estimated based on the slope of the linear fit of the $\ln(C_0/C)$ vs t graph (Figure 9). As expected, the synthesized CQDs were catalytically active for the photodegradation of methylene blue (MB). All samples displayed a linear behavior and exhibited R^2 values around 0.98 for the degradation of the methylene blue dye (Figure 9), except for the sample M4 under a tungsten 40 W lamp (W lamp), which didn't show significant changes on the concentration of the MB. Besides, sample M8 displayed the second lowest rate constant, given that samples M4 and M8 were synthesized in the absence of any hydrolyzing agent (urea) or acidic compound (nitric acid) which leaded to a poor degradation of the organic matter, resulting in relatively large carbon structures (over a 100 nm) as it was shown in Figure 4, which doesn't correspond to the size range of a CQD. Nevertheless, when these samples were exposed to sunlight both exhibited a remarkable increment on their catalytic activity. This indicates that, even when the size on these carbon structures doesn't correspond to that of the CQDs the photodegradation can be activated possibly due to an electron-hole pair on the surface of the carbon structure, that due to its size the crystal structure effects can be enhanced.

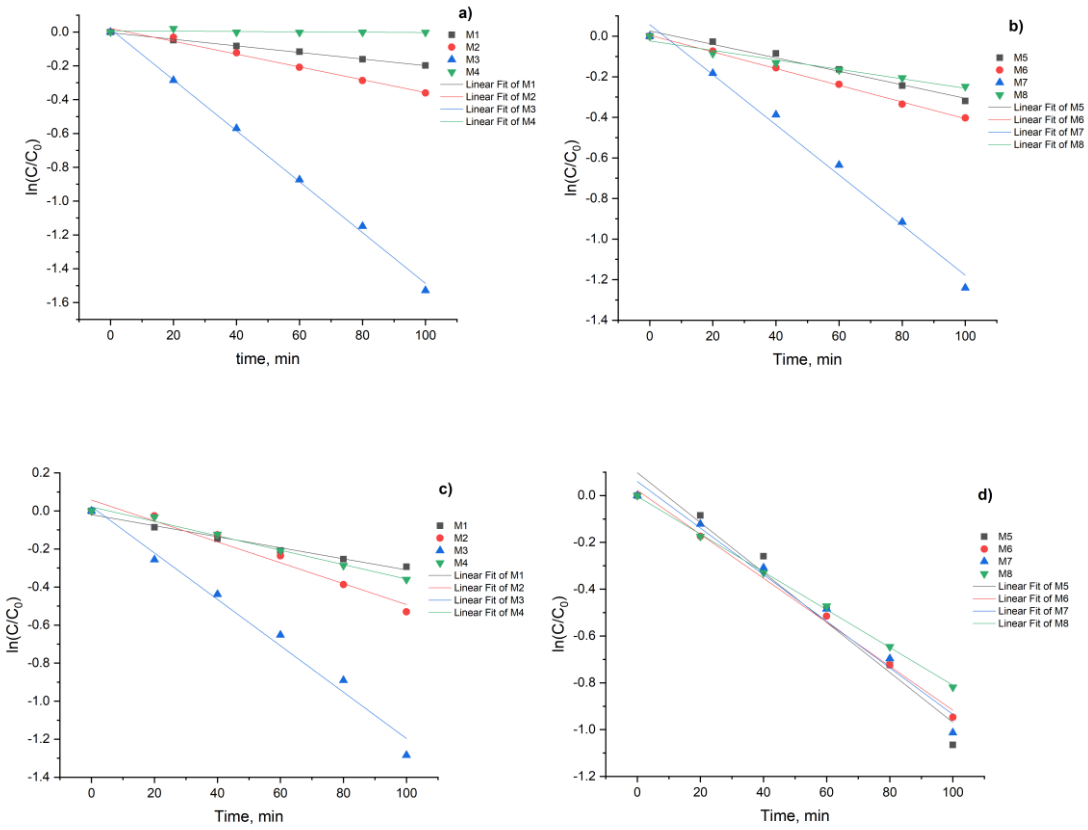

Figure 9. First order adjustment for MB photodegradation for a) Grape pomace W lamp, b) Grape pomace sunlight, c) Watermelon peel W lamp and d) Watermelon peel sunlight.

The expected mechanism for the photodegradation of MB is related with the formation of electron-hole pairs that, due to their oxidizing properties, promotes the formation of OH^- radicals, these species are responsible for the mineralization of the MB molecule[38]. Other aspects that contribute to the MB degradation, are the adsorption capacity of MB on the photocatalyst surface (CQD) and the specific surface area of the CQDs.

All samples (but M3 and M7) presented a similar behavior, increasing their photocatalytic activity when exposed to the sunlight in comparison with their performance under incandescent lamp. It is commonly known that sunlight emission spectrum presents a higher intensity at the ultraviolet range if compared with the tungsten lamp emission spectrum, considering that the band gap of the CQDs, we can affirm that sunlight does create electron-hole pairs more efficiently than the incandescent lamp, which increases the photocatalytic activity of the CQDs.

On the other hand, samples M3 and M7 displayed an opposed behavior, decreasing their photocatalytic activity when exposed to sunlight in comparison to W lamp. Both samples were prepared under the same conditions but

using two different sources of biomass. As nitric acid was used during the synthesis, it is expected the presence of C-N groups on the as synthesized CQDs, this was confirmed by FTIR spectroscopy (Fig. 5). According to the reported by Rani in 2018[39], the presence of heteroatoms into the CQDs such as oxygen, sulfur and nitrogen leads to inter-band states which decreases the recombination speed of the electron-hole pairs. Such delay enhances the photodegradation rate, which was observed for both samples (M3 and M7) independently from the nature of the biomass source.

Considering that, methylene blue molecule contains azo bonds consisting in double bonds (-N=N-), is possible to foresee a strong interaction with the C-N groups on the surface of species M3 and M7. On the other hand, such C-N groups could cause a shift in the electronic energy states[39], which facilitates the formation of electron-hole pairs when irradiated with a W lamp, resulting in a higher photocatalytic activity in comparison with the sunlight irradiation.

Even when samples M2 and M6 were synthesized using also nitric acid, the formation of C-N groups on their surfaces could be attenuated by the urea (also used during this synthesis), given that above 90ºC urea decomposes forming basic species that can partially neutralize the acidity of the nitric acid.

Additionally, the samples with smaller sizes (ranging from 1 to 10 nm) as determined by DLS, display higher catalytic activity. Specifically, samples M4 and M8 synthesized from grape pomace and watermelon, respectively, show considerable catalytic activity under sunlight irradiation. However, when analyzed under incandescent light, these samples exhibit very low activity, likely due to their specific chemical composition and the variations in light intensity between the two light sources. The comparison of the kinetic rate constant (k) showing the catalytic activity are shown in figure 10.

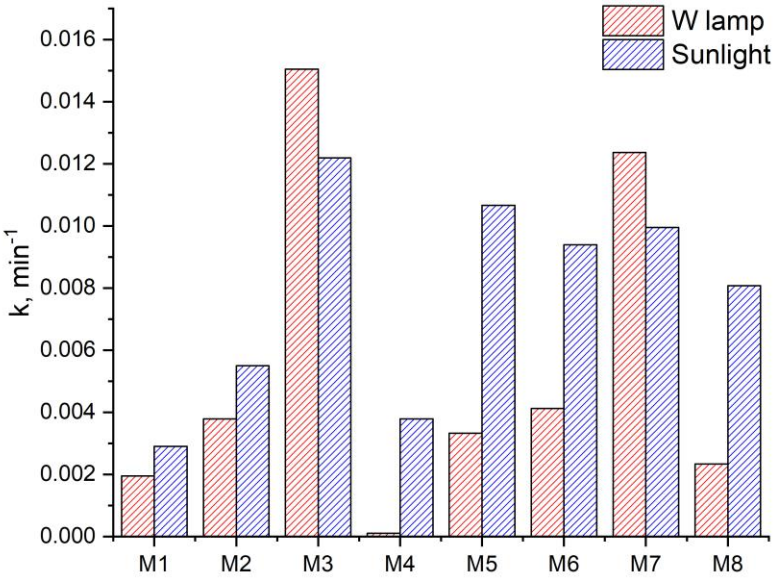

Figure 10. Graphs of the evaluation and comparison of the catalytic activity of CQDs synthesized from grape pomace and watermelon peel. (a) sunlight radiation in blue, b) light radiation with incandescent focus in red

Finally, in Figure 11, the percentages of degradation achieved for each of the catalysts under the irradiation of the two types of light are presented. These results confirm that sample 3 synthesized from grape pomace exhibits the highest level of degradation, reaching 78% under incandescent light and 72% under sunlight. Thus, it demonstrates superior activity compared to other reported CQDs used as catalysts, such as the nanomaterials obtained from uchuva and luminol.

a

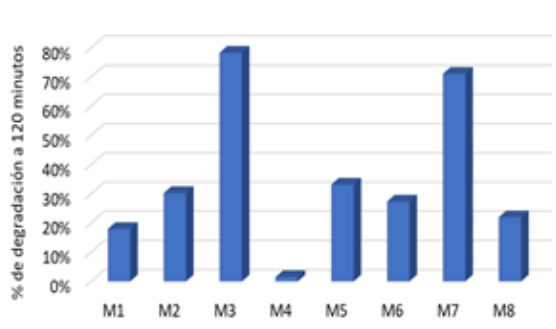

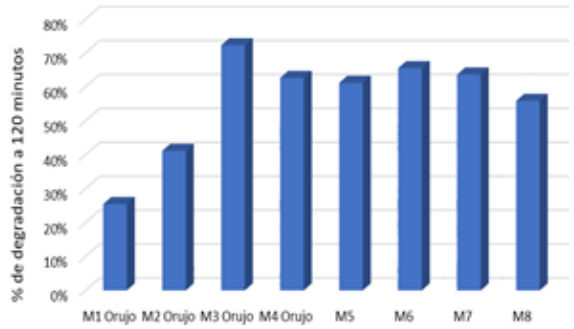

b

Figure 11. Graphs of the percentage of catalytic activity that presented the CQDs to be used as catalysts in the degradation of methylene blue dye, a) incandescent light and b) solar light.

Conclusions

Luminescent and stable carbon quantum dots (CQDs) were successfully synthesized from biomass using the hydrothermal method. Optimized synthesis parameters yielded CQDs with diverse chemical characteristics. Notably, samples derived from grape pomace and watermelon peels, synthesized with nitric acid, exhibited the highest catalytic activity in methylene blue degradation, along with enhanced luminescence and stability in comparison with the CQDs synthetized with urea. FTIR analysis confirmed the presence of desired bonds, while the catalytic evaluation highlighted consistent linear behavior, with CQDs from grape pomace peel with nitric acid displaying the highest activity overall. Solar light proved more effective than incandescent light in catalyzing reactions, and DLS results indicated that CQDs with high catalytic activity consistently fell within the 1-10 nm size range.

The luminescence activity was assessed, revealing that the CQDs displayed both upconversion and downconversion luminescence. Upconversion emerges as a highly asset for biomedical imaging, owing to the potential biocompatibility of CQDs with biological elements. Their applications span from the targeted identification of specific cell types, achieved through proper functionalization, to facilitating drug delivery. However, further investigation is required to draw a valid conclusion.

The study underscores the efficacy of the top-down hydrothermal method for CQD production, offering insights for tailored applications and emphasizing the potential of biomass-derived nanomaterials in environmental remediation

Acknowledgments

The authors wish to acknowledge the support of CETYS University and the Centro de Nanociencias y Nanotecnologia (CNyN) of UNAM for the technical support.

Conflicts of Interest

The authors declare no conflict of interest.

References

(1) Sun, X.; Lei, Y. *TrAC - Trends in Analytical Chemistry* **2017**, 163–180. doi:10.1016/j.trac.2017.02.001

(2) Velasco, L.; Ania, C. *Materiales de Carbono En Fotocatálisis*; 2011

(3) Tang, L.; Ji, R.; Cao, X.; Lin, J.; Jiang, H.; Li, X.; Teng, K. S. *ACS Nano* **2012**, *6*, 5102–5110

(4) Tang, L.; Ji, R.; Cao, X.; Lin, J.; Jiang, H.; Li, X.; Teng, K. S.; Luk, C. M.; Zeng, S.; Hao, J.; Lau, S. P. *ACS Nano* **2012**, *6*, 5102–5110. doi:10.1021/nn300760g

(5) Frasco, M. F.; Chaniotakis, N. *Sensors* **2009**, 7266–7286. doi:10.3390/s90907266

(6) SalmanOgli, A.. *Cancer Nanotechnology* **2011**, 1–19. doi:10.1007/s12645-011-0015-7

(7) Wu, H. F.; Gopal, J.; Abdelhamid, H. N.; Hasan, N. Quantum Dot Applications Endowing Novelty to Analytical Proteomics. *Proteomics* **2012**, 2949–2961. doi:10.1002/pmic.201200295

(8) Wu, H. F.; Gopal, J.; Abdelhamid, H. N.; Hasan, N. Quantum Dot Applications Endowing Novelty to Analytical Proteomics. *Proteomics*. **2012**, 2949–2961. doi:10.1002/pmic.201200295

(9) Demchenko, A. P.; Dekaliuk, M. O. *Methods and Applications in Fluorescence*. **2013**. doi:10.1088/2050-6120/1/4/042001

(10) Li, H.; Kang, Z.; Liu, Y.; Lee, S. T. *J Mater Chem* **2012**, *22*, 24230–24253. doi:10.1039/c2jm34690g

(11) Kang, C.; Huang, Y.; Yang, H.; Yan, X. F.; Chen, Z. P. *Nanomaterials*. MDPI, **2020**, 1–24. doi:10.3390/nano10112316

(12) Jusuf, B. N.; Sambudi, N. S.; Isnaeni, I.; Samsuri, S. *J Environ Chem Eng* **2018**, *6*, 7426–7433. doi:10.1016/j.jece.2018.10.032

(13) Wang, Q.; Liu, X.; Zhang, L.; Lv, Y. *Analyst* **2012**, *137*, 5392–5397. doi:10.1039/C2AN36059D

(14) Shahraki, H. S.; Bushra, R.; Shakeel, N.; Ahmad, A.; Quratulen; Ahmad, M.; Ritzoulis, C. *Journal of Bioresources and Bioproducts* **2023**. doi:10.1016/j.jobab.2023.01.009

(15) Tyagi, A.; Tripathi, K. M.; Singh, N.; Choudhary, S.; Gupta, R. K. *RSC Adv* **2016**, *6*, 72423–72432. doi:10.1039/c6ra10488f

(16) De, B.; Karak, N. *RSC Adv* **2013**, *3*, 8286–8290. doi:10.1039/c3ra00088e

(17) Sahu, S.; Behera, B.; Maiti, T. K.; Mohapatra, S. *Chemical Communications* **2012**, *48*, 8835–8837. doi:10.1039/c2cc33796g

(18) Sanchez-Sanchez, A.; Izquierdo, M. T.; Mathieu, S.; González-Álvarez, J.; Celzard, A.; Fierro, V. *Green Chemistry*, **2017**, 2653-2665

(19) Liu, H.; Ye, T.; Mao, C. *Angewandte Chemie* **2007**, *119*, 6593–6595. doi:10.1002/ange.200701271

(20) Prasannan, A.; Imae, T. *Industrial and Engineering Chemistry Research*; **2013**; Vol. 52, 15673–15678. doi:10.1021/ie402421s

(21) Kailasa, S. K.; Bhamore, J. R.; Koduru, J. R.; Park, T. J. Chapter 11, *Biomedical Applications of Nanoparticles*; Grumezescu, A. M., Ed.; William Andrew Publishing, **2019**; 295–317. doi:https://doi.org/10.1016/B978-0-12-816506-5.00006-1

(22) Shen, J.; Zhu, Y.; Yang, X.; Li, C. *Chemical Communications* **2012**, *48*, 3686–3699. doi:10.1039/c2cc00110a

(23) Hu, C.; Li, M.; Qiu, J.; Sun, Y.-P. *Chem Soc Rev* **2019**, *48*, 2315–2337. doi:10.1039/C8CS00750K

(24) Li, H.; Kang, Z.; Liu, Y.; Lee, S. T. *J Mater Chem* **2012**, *22*, 24230–24253. doi:10.1039/c2jm34690g

(25) Haryadi, H.; Purnama, M. R. W.; Wibowo, A. *Indonesian Journal of Chemistry* **2018**, *18*, 594. doi:10.22146/ijc.26652

(26) Zhang, R.; Liu, Y.; Yu, L.; Li, Z.; Sun, S. *Nanotechnology* **2013**, *24*. doi:10.1088/0957-4484/24/22/225601

(27) Cheng, C.; Shi, Y.; Li, M.; Xing, M.; Wu, Q. *Materials Science and Engineering C* **2017**, *79*, 473–480. doi:10.1016/j.msec.2017.05.094

(28) Houas, A.; Lachheb, H.; Ksibi, M.; Elaloui, E.; Guillard, C.; Herrmann, J. M. *Appl Catal B* **2001**, *31*, 145–157. doi:10.1016/S0926-3373(00)00276-9

(29) Liu, H.; Ye, T.; Mao, C. *Angewandte Chemie* **2007**, *119*, 6593–6595. doi:10.1002/ange.200701271

(30) Yuan, M.; Zhong, R.; Gao, H.; Li, W.; Yun, X.; Liu, J.; Zhao, X.; Zhao, G.; Zhang, F. *Appl Surf Sci* **2015**, *355*, 1136–1144. doi:10.1016/j.apsusc.2015.07.095

(31) Remli, U. R. R. P.; Aziz, A. A. *IOP Conference Series: Materials Science and Engineering*; Institute of Physics Publishing, **2020**; Vol. 736. doi:10.1088/1757-899X/736/4/042038

(32) Habiba, K.; Makarov, V. I.; Avalos, J.; Guinel, M. J. F.; Weiner, B. R.; Morell, G. *Carbon N Y* **2013**, *64*, 341–350. doi:10.1016/j.carbon.2013.07.084

(33) Dhenadhayalan, N.; Lin, K. C.; Suresh, R.; Ramamurthy, P. *Journal of Physical Chemistry C* **2016**, *120*, 1252–1261. doi:10.1021/acs.jpcc.5b08516

(34) Zhu, X.; Xiao, X.; Zuo, X.; Liang, Y.; Nan, J. *Particle & Particle Systems Characterization* **2014**, *31*, 801–809. doi:https://doi.org/10.1002/ppsc.201300375

(35) Sk, M. A.; Ananthanarayanan, A.; Huang, L.; Lim, K. H.; Chen, P. *J Mater Chem C Mater* **2014**, *2*, 6954–6960. doi:10.1039/C4TC01191K

(36) Demchenko, A. P.; Dekaliuk, M. O. *Methods and Applications in Fluorescence*. IOP Publishing Ltd December 1, 2013. doi:10.1088/2050-6120/1/4/042001

(37) Zhu, S.; Song, Y.; Wang, J.; Wan, H.; Zhang, Y.; Ning, Y.; Yang, B. *Nano Today* **2017**, *13*, 10–14. doi:10.1016/j.nantod.2016.12.006

(38) Zhuo, S.; Shao, M.; Lee, S.-T. *ACS Nano* **2012**, *6*, 1059–1064. doi:10.1021/nn2040395

(39) Chou, K. F.; Dennis, A. M. *Sensors (Switzerland)* **2015**, *15*, 13288–13325. doi:10.3390/s150613288